5A.4

POLARIMETRIC VARIABILITY OF SUPERCELL STORMS IN SIMILAR ENVIRONMENTS

Matthew S. Van Den Broeke

Department of Earth and Atmospheric Sciences, University of Nebraska-Lincoln, Lincoln, Nebraska

ABSTRACT

Classic supercell storms exhibit large variability among different environments. Of interest is whether changes to environmental variables, such as the vertical wind and moisture profiles, are manifest as repeatable microphysical patterns. These microphysical patterns may be studied using polarimetric weather radar. In this study, classic supercell storms were identified in similar environments, and compared to other sets of storms in different environments. Generally, features of the storms such as differential reflectivity (Z_{DR}) columns and arcs exhibited greater similarity among storms in the same environment than across environments, though there were exceptions. For instance, areal extent of the 3.5-dB Z_{DR} arc was *not* very similar between storms in similar environments, whereas width and mean values in the Z_{DR} arc *were* relatively similar between storms in similar environments. These results indicate that some radar features of supercell storms may be used to learn about microphysical variation across environments, while others may not be as useful.

Corresponding author address: Matthew Van Den Broeke,
Dept. of Earth and Atmospheric Sciences, University of Nebraska-Lincoln,
Lincoln, NE, 68588
Email: mvandenbroeke2@unl.edu

1. Introduction

Polarimetric weather radar can be used to infer properties of scatterers such as their orientation, phase, and shape. Thus, the polarimetric variables offer a unique opportunity to study microphysical processes within clouds, including those which produce substantial human impacts.

In this study, we focus on classic supercell storms (e.g., Moller et al. 1994). These storms have well-known radar signatures (e.g., Kumjian and Ryzhkov 2008; Romine et al. 2008; Van Den Broeke et al. 2008; Kumjian et al. 2010). These signatures are typically visible using reflectivity factor (Z_{HH}), differential reflectivity (Z_{DR}), and/or copolar cross-correlation coefficient (ρ_{hv}), and include a few of special focus herein:

1) Z_{DR} columns: in any strong updraft, liquid drops may be lofted above the ambient 0°C level. These drops are visible as a region of relatively high Z_{DR} values aloft. Given the strong updrafts common in supercell storms, Z_{DR} columns are often well-defined (e.g., Brandes et al. 1995; Kumjian et al. 2010).
2) Z_{DR} arcs: strong inflow toward the supercell updraft often leads to a zone of sorting along the supercell forward flank. Large drops are common in this region, leading to relatively high Z_{DR} values. This feature arises as rain and hail are sorted, and aligns with the average storm-relative wind in a deep layer (e.g., Dawson et al. 2014).
3) Preferred area of hailfall: many supercell storms produce hail, though the region of hailfall varies substantially between storms in terms of magnitude and placement. The region of hailfall may be identified by an area of collocated high Z_{HH} and low Z_{DR} values in or near the storm core. This area often exhibits cyclicality, which may be related to the tornado life cycle (e.g., Van Den Broeke et al. 2008).

A broad research goal is to understand how supercell microphysics vary as a function of environmental conditions, using radar features as metrics. To be able to use these features to study microphysical changes arising from environmental variability, it is important to know if storms in similar environments exhibit similar radar signatures. Specifically, working in this direction, this research represents an initial attempt to quantify the similarity between radar signatures of classic supercell storms in similar environments, and to determine the magnitude of these variations across environments. If the variation is less in similar environments than across a set of environments for a particular supercell feature, that feature may be useful in future studies of microphysical variability as a function of environment.

2. Methods and Data

From a large database of supercell storms, relatively short time periods (< 2-3 hours) were sought during which multiple well-structured classic supercell storms were present, and during which the environment did not appear to appreciably change. Environments were required to be characterized by low spatial variability, e.g., no frontal or outflow boundaries could be present. Events were also preferred in which storms analyzed were close enough to the radar that the base-scan altitude within them was <1 km for a substantial portion of the analysis period. For each storm chosen for analysis, the analysis period was defined such that well-defined classic supercell structure was present, including appreciable cyclonic rotation at midlevels (left-moving storms were not included), an echo appendage in some form, and a Z_{DR} column and arc. When initially chosen, no weight was given to whether an environment was tornadic or non-tornadic; both categories were present in the final set of storms selected. The list of days selected, the radar used for each, and the number of sample volumes analyzed is presented in Table 1.

Table 1: Events used for the analysis described in this paper. #Storms denotes the number of storms analyzed from a particular day, and #Volumes indicates the number of individual sample volumes analyzed in sum from a particular radar. The last column indicates whether or not one or more tornado reports were associated with the environment (though not necessarily with each storm in the sample).

Date	Radar	#Storms	#Volumes	Tornadic?
3-2-12	KHTX	2	30	Yes
3-3-12	KFFC	2	25	Yes
4-15-12	KTWX	2	20	Yes
2-18-13	KSHV	2	14	Yes
4-17-13	KFDR	3	53	Yes
4-22/23-13	KVNX	2	21	No
4-27-13	KTLX	2	25	No
5-30-13	KTLX	2	23	No

For each event, a representative environment was selected from a RUC or RAP sounding. The sounding site was carefully selected to be representative of storm inflow, and not influenced by boundaries or other features. Satellite, radar, and surface observations were utilized to ensure the representativeness of selected soundings.

Level II radar data was obtained from the nearest polarimetric WSR-88D radar for the selected set of storms from the National Climatic Data Center (NCDC) archive. These data were analyzed as described below using NCDC's Weather and Climate Toolkit.

Since distributions of features analyzed (e.g., Z_{DR} arc areal extent) were not Gaussian, the Wilcoxon-Mann-Whitney (WMW) test was used to assess the relative similarity of storms in similar environments. In this case, the WMW test was used to assess whether the values from two storms could have been drawn from the

same population, e.g., could have occurred in the same storm. *High* p-values indicate that the populations from two storms are likely to have come from the same population. This is opposite the usual application of WMW statistics, in which *low* p-values are used to indicate that two populations are likely to be separate.

3. Results

a. Updraft Signatures

Environmental variables are known to influence updraft characteristics of numerically-simulated supercell storms. For instance, Gilmore et al. (2004) found that in simulations with stronger vertical wind shear, updraft of simulated storms were larger in areal extent and tended to be stronger. Z_{DR} columns can be used to infer updraft strength and broadness, since they represent liquid drops being lofted within the updraft. Broadness of the Z_{DR} column is closely related to broadness of the updraft (at least that portion of the updraft where the temperature is relatively warm compared to ambient conditions), and maximum altitude of the Z_{DR} column may be related to updraft strength, since a stronger (and possibly warmer) updraft will be required to loft liquid drops to greater altitude. Updraft broadness has also been related to updraft strength (e.g., Kumjian et al. 2010).

A measure of updraft strength used in this analysis is the maximum altitude of the 1-dB Z_{DR} column in the supercell updraft region. A threshold of 1 dB was used to reduce the effects of noise in the data, and to overcome the Z_{DR} biases inherent to WSR-88D data (e.g., Zittel et al. 2014). Mean values of this metric for each storm analyzed are shown in Fig. 1.

Figure 1: Mean values of maximum 1-dB Z_{DR} column height (km) across all analysis periods for each storm. Each bar represents one storm, and each group of bars of the same color represents all storms in the same environment.

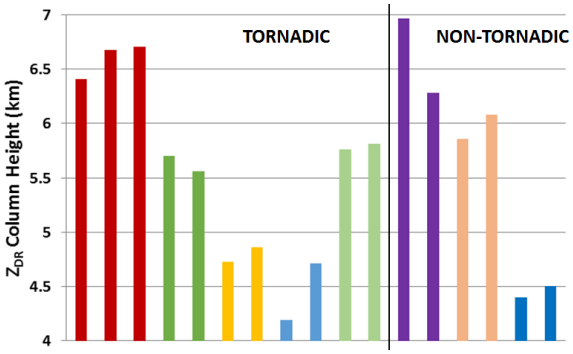

Storms in similar environments tend to have relatively similar mean Z_{DR} column maximum altitudes, indicated by the relatively similar height of the same-colored bars in Fig. 1. These similarities are supported by p-values from the WMW test (Table 2). Tornadic and non-tornadic storms are not strongly differentiated in this small sample.

Table 2: WMW p-values for Z_{DR} column maximum altitudes in storms in similar environments, for environments containing 2 individual storms. P-values calculated using the population of all values for each storm. As noted in Methods, relatively *high* p-values indicate that the populations of Z_{DR} column altitudes from different storms in the same environment could have been observed from a single storm.

Storm Events	p, compared to other storm in same environment
D, E	0.330
H, I	0.198
L, M	0.078
N, O	0.468
1, 2	0.074
3, 4	0.109
5, 6	0.401

Thus, from this initial sample of cases, it appears that Z_{DR} column maximum altitude is a relatively similar metric across storms in the same environment. Future analysis will determine whether values are significantly different across environments examined. Maximum Z_{DR} column altitude for a given environment was relatively strongly related to most unstable convective available potential energy (muCAPE; r^2 ~0.46) and effective storm-relative helicity (ESRH; r^2 ~0.45), with increasing CAPE and helicity corresponding to increasing Z_{DR} column altitude.

A metric used to estimate updraft broadness was areal extent of the 0.5-dB Z_{DR} column (km^2) above the ambient 0°C level. Areal extent was calculated using a GIS approach. Altitude was approximately 1 km above the ambient 0°C level; 0.75 km – 1.25 km was used so that a datapoint could be added for most sample volumes (e.g., in some sample volumes, spacing of successive beam centerlines precluded the choice of any representative areal extent value, as none fell within the 0.75 – 1.25 km range). Mean updraft broadness values are shown in Fig. 2.

Figure 2: As in Fig. 1, except bars represent mean value (km^2) of the 0.5-dB Z_{DR} column areal extent at 0.75 – 1.25 km above the ambient 0°C level.

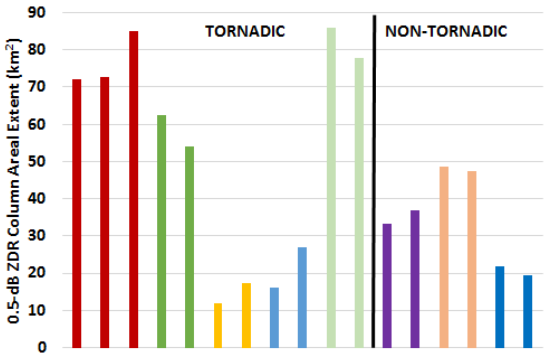

Storms in similar environments again appear to have fairly similar mean values of Z_{DR} column areal extent. This is again supported by the results of WMW tests of significance (Table 2). Again, tornadic and non-tornadic storms are not strongly differentiated.

Table 2: As in Table 1, except for Z_{DR} column areal extent above the ambient 0°C level.

Storm Events	p, compared to other storm in same environment
D, E	0.131
H, I	0.030
L, M	0.136
N, O	0.189
1, 2	0.171
3, 4	0.464
5, 6	0.484

Thus, Z_{DR} column areal extent, at least at this particular altitude above the ambient 0°C level, also appears to be a relatively similar metric across storms in a similar environment. This metric was best-correlated with altitude of the ambient 0°C level ($r^2 \sim 0.73$). Higher-altitude 0°C levels were strongly associated with larger Z_{DR} columns at a fixed level above the ambient 0°C level. A very warm environment below appears to be associated with large Z_{DR} columns. muCAPE was not strongly predictive of Z_{DR} column areal extent ($r^2 \sim 0.29$).

b. Inflow Signatures

Size sorting of hail and raindrops along a supercell forward flank depends on the mean storm-relative wind over the depth of the sorting layer (Dawson et al. 2015). This size sorting leads to the development of a band of large drops, marked by high Z_{DR} values, in that location. Thus, characteristics of the Z_{DR} arc should be instructive of the storm-scale wind profile, and have been related to the tornado life cycle (e.g., Palmer et al. 2011; Crowe et al. 2012).

Mean width of the 2-dB Z_{DR} arc was one characteristic investigated (Fig. 3), measured perpendicular to the forward flank. Z_{DR} arc width, and separation from the storm core, may be a means of estimating storm-relative wind shear at low levels (Ganson and Kumjian 2015).

Figure 3: As in Fig. 1, except for mean width of the 2-dB Z_{DR} arc.

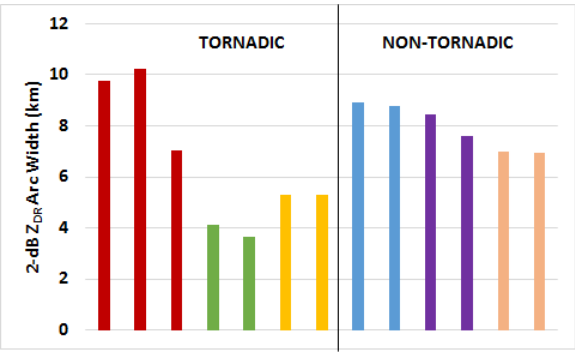

More variability may be present for this metric, though storms in similar environments generally have similar mean Z_{DR} arc width values. Non-tornadic storms, in this sample, tended to have wider Z_{DR} arcs. Z_{DR} arc width was not strongly related to environmental variables included in the analysis. For the entire sample of storm environments, the coefficient of determination for ESRH was only $r^2 \sim 0.07$, though when one outlier environment was removed, $r^2 \sim 0.38$. Larger ESRH values were typically associated with wider Z_{DR} arcs.

Areal extent of the Z_{DR} arc was also investigated, as variations thereof have been related to the tornado life cycle (e.g., Palmer et al. 2011; Crowe et al. 2012). A threshold of 3.5 dB was used, which was somewhat arbitrary but captured well the region of the arc dominated by very high values, and was substantially different through time (e.g., a lower threshold would have led to less temporal variability, and may have been less sensitive to subtle changes in the storm-relative shear). This metric was also calculated using a GIS approach. Mean Z_{DR} arc areal extent is shown in Figure 4.

Figure 4: As in Fig. 1, except for mean areal extent of the 3.5-dB Z_{DR} arc.

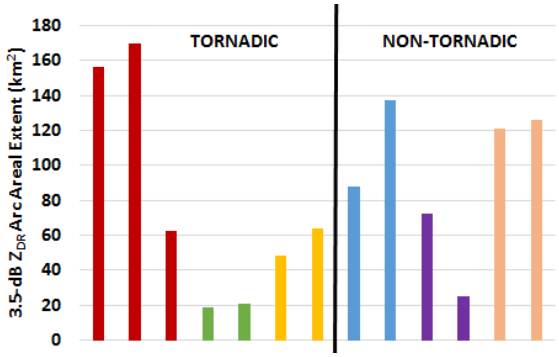

Variability is substantial between storms in similar environments. For example, the red bars, blue bars, and purple bars in Fig. 4 show quite different values of mean Z_{DR} arc areal extent. It is unknown if this variability is sensitive to the choice of Z_{DR} threshold used to define the arc region. From these preliminary results, it appears that Z_{DR} arc areal extent may be a less-applicable variable when studying environmental influences on supercell microphysics. Tornadic and non-tornadic environments were not well-differentiated, though a few storms in non-tornadic environments were associated with large Z_{DR} arc widths. This finding warrants study with a larger sample of environments. Z_{DR} arc width was not closely related to any environmental variables included in the analysis.

A third metric related to the Z_{DR} arc was the mean value of all pixels within the Z_{DR} arc with values exceeding 0 dB. These collections of pixel values were concatenated across all sample volumes analyzed for a given storm. Distributions of Z_{DR} arc pixels were generally Rayleigh, with a variable peak usually between 2-4 dB and a long right tail extending to the maximum allowable value (~7.9 dB). Mean Z_{DR} arc values for the storms analyzed are shown in Fig. 5.

Figure 5: As in Fig. 1, except for mean value of all pixels within the Z_{DR} arc region.

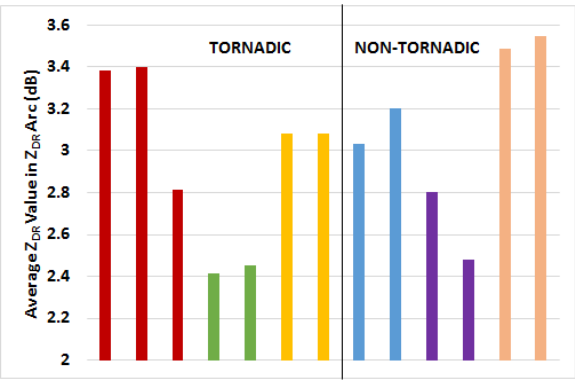

In general, values were similar between storms in similar environments. Tornadic and non-tornadic storms were not strongly differentiated. The strongest association between Z_{DR} arc mean value and an environmental variable was with level of free convection (LFC) height ($r^2 \sim 0.45$). It is speculated that storms in high-LFC environments may be associated with much evaporation below the LFC level, leading to larger drops initially present even before sorting can act to create the Z_{DR} arc.

c. Hailfall Characteristics

Hail produced in supercell updrafts may fall out downstream from the updraft region, and sometimes falls out on the west side of the mesocyclone. Hailfall is rarely steady through time in supercell storms, but more commonly exhibits cyclicality (e.g., Van Den Broeke et al. 2008). Non-tornadic storms may exhibit less hailfall cyclicality (Kumjian and Ryzhkov 2008). Magnitude of the region receiving hailfall seems to vary substantially between storms, but this has not been quantified and related to environmental variables.

As an initial metric related to hailfall, areal extent of the polarimetrically-inferred hailfall region was examined, calculated using a GIS approach. Area was calculated for the base scan, for scans <1 km in altitude. Hail was polarimetrically inferred by the collocation of locally-enhanced Z_{HH} values and locally-reduced Z_{DR} values (where Z_{DR} values typically ranged from -0.5 to +1 dB). These results are shown in Fig. 6.

Figure 6: As in Fig. 1, except for mean polarimetrically-inferred hail areal extent (km^2) at base-scan level.

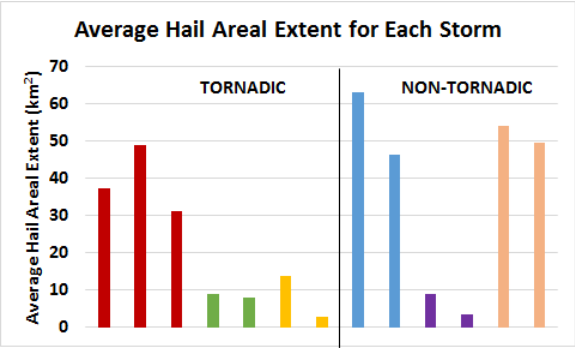

Variability was substantial between storms in the same environment, with areal extent populations from two storms in the same environment more likely to indeed appear as though they were from two separate storms (Table 3). Non-tornadic storms were often characterized by large values of hail areal extent, though a larger sample would be needed to determine if this is more broadly true. It is not known, at this time, if the higher values in non-tornadic storms were a result of relative lack of cyclicality (e.g., more analysis periods had large areas of hailfall, leading to a higher mean) or if hailfall regions simply tended to be larger in these non-tornadic storms.

Table 3: As in Table 1, except for polarimetrically-inferred hailfall areal extent in base-scan data.

Storm Events	p, compared to other storm in same environment
H, I	0.154
L, M	0.002
1, 2	0.016
5, 6	0.480

Hailfall areal extent was fairly well-predicted by LFC height (r^2 ~ 0.53), with higher-altitude LFCs associated with larger hailfall regions. It is speculated that this association may exist partially because of greater low-level evaporation in high-LFC environments, since greater evaporative and associated cooling leads to less loss of ice mass through melting. Temperature at the lifting condensation level (LCL) was not as good of a predictor (r^2 ~ 0.21).

Hailfall cyclicality was also briefly investigated, given the potential association with tornadic vs. non-tornadic storms. The measure of cyclicality used was (standard deviation of hailfall areal extent) divided by (mean hailfall areal extent) for each storm. Thus, higher values indicate greater cyclicality. In this relatively small sample, tornadic storms generally did tend to experience more cyclic hailfall (Fig. 7), though there was overlap with non-tornadic storms.

Figure 7: As in Fig. 1, except for mean standard deviation divided by mean hailfall areal extent in base scan. Greater values indicate greater hailfall cyclicality.

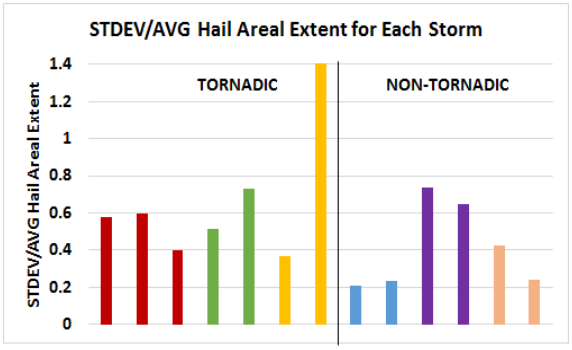

A final hailfall-related measure was hail fallout location. This measure was assessed from base-scan data, given that the entire region of hail fallout was located at an altitude <1 km. Hail placement was defined as the centroid of the hail fallout region relative to the midlevel mesocyclone center. The midlevel scan was defined as the scan within or nearest the 2.5-3 km altitude. Mesocyclone-relative hail fallout locations are shown in Fig. 8.

Figure 8: Location of base-scan hail fallout centroid relative to the midlevel (2.5-3 km) mesocyclone. Each dot represents one sample volume, and dots of the same color represent storms in similar environments. Range rings in km outward from the mesocyclone center.

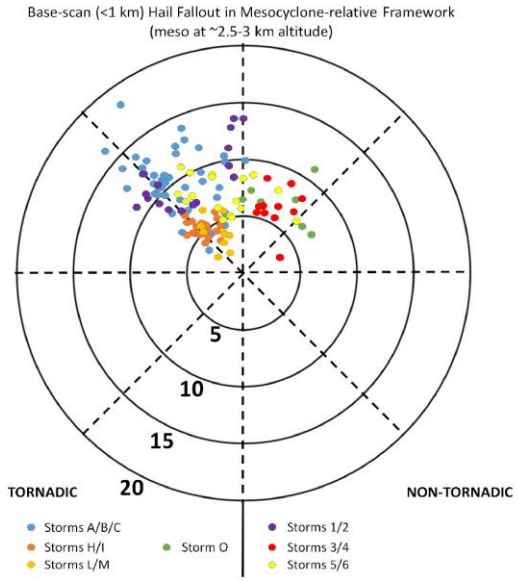

The points tend to cluster, indicating that mesocyclone-relative hail fallout location is sensitive to environmental variables. Here, no work was done to assess which environmental variables may be the most important to hail fallout location. It was noted that non-tornadic storms often exhibited greater variation in placement, whereas hail fallout locations for tornadic storms were often more tightly clustered. These results are intriguing and warrant future work.

4. Conclusions and Future Work

In this preliminary work, some polarimetric metrics appear reasonably similar between storms in similar environments, and reasonably different between environments. These metrics include Z_{DR} column maximum altitude and areal extent, Z_{DR} arc width and mean values, and hailfall areal extent and fallout location. These metrics may be especially useful in future studies examining the effects of changing environments on supercell microphysics. Further study is required, however, to further quantify the preliminary associations discovered here.

Other polarimetric metrics were not very similar between storms in similar environments. These included areal extent of the 3.5-dB Z_{DR} arc, and possibly base-scan hailfall cyclicality. While these variables may be less useful to future supercell microphysical studies, further work is warranted to see if these preliminary results hold with a larger sample of storms, and/or if modified thresholds (e.g., 3.5 dB for the Z_{DR} arc) might yield more useful information.

Taken as a whole, these preliminary results may indicate substantial utility in using polarimetric radar signatures of supercell storms to study effects of environmental variability on supercell microphysics.

ACKNOWLEDGEMENTS

Lena Heuscher, Sabrina Jauernic, and Nicholas Humrich helped gather environmental data associated with the larger supercell dataset. The author wishes to acknowledge the University of Nebraska-Lincoln for regular academic year support.

REFERENCES

Brandes, E. A., J. Vivekanandan, J. D. Tuttle, and C. J. Kessinger, 1995: A study of thunderstorm microphysics with multiparameter radar and aircraft observations. *Mon. Wea. Rev.*, **123**, 3129-3143.

Crowe, C. C., C. J. Schultz, M. Kumjian, L. D. Carey, and W. A. Petersen, 2012: Use of dual-polarization signatures in diagnosing tornadic potential. *Elec. J. Operational Meteor.*, **13(5)**, 57-78.

Dawson, D. T., E. R. Mansell, Y. Jung, L. J. Wicker, M. R. Kumjian, and M. Xue, 2014: Low-level Z_{DR} signatures in supercell forward flanks: The role of size sorting and melting of hail. *J. Atmos. Sci.*, **71**, 276-299.

Dawson, D. T., E. R. Mansell, and M. R. Kumjian, 2015: Does wind shear cause hydrometeor size sorting? *J. Atmos. Sci.*, **72**, 340-348.

Ganson, S. M., and M. R. Kumjian, 2015: Quantifying the relationship between the Z_{DR} arc signature and low-level vertical wind shear. *37th Conference on Radar Meteorology*, Norman, Oklahoma, Amer. Meteor. Soc.

Gilmore, M. S., and L. J. Wicker, 1998: The influence of midtropospheric dryness on supercell morphology and evolution. *Mon. Wea. Rev.*, **126**, 943-958.

Kumjian, M. R., and A. V. Ryzhkov, 2008: Polarimetric signatures in supercell thunderstorms. *J. Appl. Meteor. Climatol.*, **47**, 1940-1961.

Kumjian, M. R., A. V. Ryzhkov, V. M. Melnikov, and T. J. Schuur, 2010: Rapid-scan super-resolution observations of a cyclic supercell with a dual-polarization WSR-88D. *Mon. Wea. Rev.*, **138**, 3762-3786.

Moller, A. R., C. A. Doswell III, M. P. Foster, and G. R. Woodall, 1994: The operational recognition of supercell thunderstorm environments and storm structures. *Wea. Forecasting*, **9**, 327-347.

Palmer, R. D., D. Bodine, M. Kumjian, B. Cheong, G. Zhang, Q. Cao, H. B. Bluestein, A. Ryzhkov, T. Yu, and Y. Wang, 2011: Observations of the 10 May 2010 tornado outbreak using OU-PRIME: Potential for new science with high-resolution polarimetric radar. *Bull. Amer. Meteor. Soc.*, **92**, 871-891.

Romine, G. S., D. W. Burgess, and R. B. Wilhelmson, 2008: A dual-polarization-radar-based assessment of the 8 May 2003 Oklahoma City area tornadic supercell. *Mon. Wea. Rev.*, **136**, 2849-2870.

Van Den Broeke, M. S., J. M. Straka, and E. N. Rasmussen, 2008: Polarimetric radar observations at low levels during tornado life cycles in a small sample of classic Southern Plains supercells. *J. Appl. Meteor. Climatol.*, **47**, 1232-1247.

Zittel, W. D., J. G. Cunningham, R. R. Lee, L. M. Richardson, R. L. Ice, and V. Melnikov, 2014: Use of hydrometeors, Bragg scatter, and sun spikes to determine system Z_{DR} biases in the WSR-88D fleet. *8th European Conference on Radar in Meteorology and Hydrology*, Garmisch-Partenkirchen, Germany, Deutscher Wetterdienst/German Aerospace Center.